

# Parallel compliance design for increasing robustness and efficiency in legged locomotion – proof of concept

Maziar Ahmad Sharbafi, Mohammad Javad Yazdanpanah, Majid Nili Ahmadabadi, and Andre Seyfarth,

**Abstract**—Benefiting from serial compliance in series elastic actuators (SEA) can be considered as a breakthrough in robotics. Recently, applying the parallel compliance in robot designs is growing based on its advantages such as reduction in consumed torques. In this paper, we aim at employing parallel compliance to increase walking robustness of bipedal robots against model uncertainties. Utilizing passive compliant elements instead of adapting the controller in order to cope with uncertainties make the system more efficient and less sensitive to measurement issues such as delays and noise. We introduce a methodology for designing both parallel compliance and controller using Hybrid Zero Dynamics (HZD) concept. This study includes simulation results representing the design approach and preliminary experiments on parallel compliance effects on efficiency of a robot joint position control. The simulations comprise a compass gait (2-link) model and a 5-link model. The ground slope and robot segment lengths are considered as uncertain parameters in the first and second models, respectively. The control target is met by insertion of compliant structures in parallel to the actuators. In order to employ the proposed method on a real robot, we suggest using pneumatic air muscles as parallel compliant elements. Pilot experiments on the knee joint of BioBiped3 robot supports the feasibility of suggested method.

## I. INTRODUCTION

Series Elastic Actuators (SEAs, [1]) provide clear benefits for artificial legged locomotor systems by adding compliance to the traditional rigid actuators (e.g., electric motors (EM)) [2], [3], [4]. In comparison with non-compliant actuators, the SEA has lower impedance, higher efficiency and robustness against perturbations [5], [6]. These advantages are obtained by restoring energy through serial elasticity of the actuator. This behavior mimics the stretch-shortening cycles in biological muscle, [7]. Furthermore, Hurst showed that adding compliance to the robot structure considerably simplifies control [8]. One step further will be stiffness adjustment in variable impedance actuators (VIA) [9] which is mainly attained by addition of a second actuator for adapting to different gait conditions (e.g., speed). Although the VIA improves the controllability of the output which is useful for enabling legged robots to cope with uncertainties and perturbations, the mechanical design and control are much more complex [9], [10] than EM and SEA. In addition, both actuators in a

VIA continuously produce torques during the movement (e.g., as in the humanoid robot Veronica [10]), and hence it can reduce the required power, but not the torque [11], [12].

Addition of a parallel compliant element to an actuator can reduce EM torque, as the joint torque does only partially pass through the motor [11], [6]. Auxiliary parallel compliance can help to achieve the required torques above the actuator limitations. By adding such parallel compliant elements, the control efforts shifts to stabilizing the motion [12]. With added parallel compliance and matching control effort, system stability and robustness against uncertainties can be improved [11]. It is also in line with muscular parallel passive compliance (epimysium and titin [13]) in biological locomotor systems [14]. In [15], the advantages of appropriate mechanical design to enhance control were shown and compared with findings in human walking. In studies on mimicking human ankle joint behavior with a prosthetic foot, Grimmer et al. showed that the required peak power and peak torque can be reduced by adding a parallel compliance [16]. With a well designed biped having human-like body characteristics (e.g., compliant muscles), a simple open loop controller can stabilize walking [17], [18].

In [19], using the concept of virtual constraint, the controller was designed with feedback linearization and the hybrid zero dynamics (HZD) method was introduced for stability analyses. Later, the compliance (as a physical constraint) was inserted to the robot joints to increase the control efficiency and the stability was investigated using HZD concept [20] and [21]. Hence, both physical and virtual adjustable impedance could be employed for design and control [22], [19], [8]. Inspired from the compliant HZD control approach, here, we introduce a method to shape motion dynamics via deliberate insertion of passive compliant elements, parallel to the robot's actuators. With that, we can simultaneously design and control a robust and efficient locomotor system.

In the following, Sec. II presents the basic concepts of modeling and the HZD control from [19]. In Sec. III, the proposed method including an algorithm to design HZD-based compliant controller is explained. The supporting theorems are presented here, but some of the proofs are described in a complementing paper [23]. Section IV comprises two simulation and one experimental results. Robustness against uncertainties in the ground slope and body parameters are targeted by simulation models (Fig. 1). The results of a pilot study on employing PAM (pneumatic artificial muscle), as adjustable compliance are described at the end of this section. Discussions and future steps are presented in Section V.

M. A. Sharbafi, M. J. Yazdanpanah and M. N. Ahmadabadi are with the Control and Intelligent Processing Center of Excellence (CIPCE) School of Electrical and Computer Engineering, University of Tehran, Tehran, Iran.

M. A. Sharbafi, and A. Seyfarth are with Laufflabor Locomotion Lab, Institute of Sport Science, Centre for Cognitive Science, TU Darmstadt, Germany.

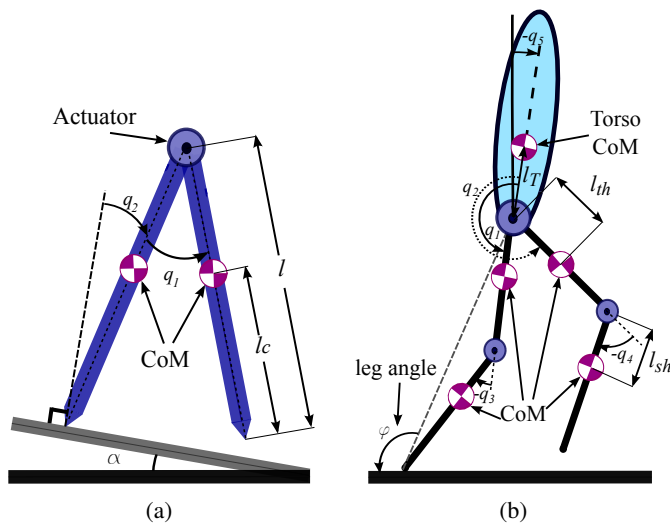


Fig. 1: Schematic and definitions of variables and parameters in (a) the Acrobot model and (b) the 5-link model.

## II. BASIC CONCEPTS

Here, we describe the hybrid zero dynamics control method after presenting a short overview of the modeling approach.

### A. Dynamic model

We consider an  $N - link$  model with point feet and without any closed chain as introduced in [19]. A hybrid model is utilized for such a system including continuous and discrete sub-phases. The single support phase, which defines the continuous part, consists of ordinary differential equations describing the motion of the robot when only one leg is in contact with the ground and the other leg swings forward. In the double support phase, a discrete subsystem models the impact when the swing leg touches the ground. Let the system states  $q = [q_1, \dots, q_N]^T$ , in which the first  $N - 1$  variables are the joint angles and the last one ( $q_N$ ) is the angle between the unactuated foot contact and the ground. Two samples are shown in Fig. 1. Since the HZD controller can be applied to models with higher degrees of underactuation [24], [15], this is also valid for our control approach.

From Lagrange equation the swing phase dynamics is determined as follows:

$$\begin{aligned} \dot{x} &= \begin{bmatrix} \dot{q} \\ D^{-1}(q)[-C(q, \dot{q})\dot{q} - G(q) + Bu] \end{bmatrix} \\ &= f(x) + g(x)u \end{aligned} \quad (1)$$

in which  $D$ ,  $C$ ,  $G$  and  $B$  are the inertia and Coriolis matrices, the gravity vector and a constant matrix that maps the joint torque vector  $u$  to the generalized forces, respectively. In addition, the state variables are defined by  $x = [q, \dot{q}]^T$ . When the swing leg hits the ground, an inelastic impact  $\Delta$  occurs. The hybrid walking model will be

$$\Sigma = \begin{cases} \dot{x} = f(x) + g(x)u & x^- \notin \mathcal{S} \\ x^+ = \Delta(x^-) & x^- \in \mathcal{S} \end{cases} \quad (2)$$

in which,  $\mathcal{S}$  is the switching surface and super-indexes  $-$  and  $+$  denote the moments exactly before and after impact, respectively.

### B. Designing HZD controller

Our control approach is utilizing hybrid zero dynamics (HZD) [25], [26] to design virtual and physical constraints. The holonomic constraints on the robot's configuration which are asymptotically achieved through the feedback control action are defined as virtual constraints,  $y = h(q)$  [27]. This virtual constraints approach has been applied very successfully in designing feedback controllers for planar bipedal robot walking with stability proof [28], [25] and [27]. In HZD control design, the control torque is determined via feedback linearization to regulate the output ( $y$ ) to zero which provides a stable attractive manifold, namely "hybrid zero dynamics manifold".

$$u(x) = (L_g L_f h(x))^{-1} \overbrace{(-K_D \dot{y} - K_P y)}^v - L_f^2 h(x) \quad (3)$$

In this equation,  $L_f h(x) := \frac{\partial h}{\partial x} f$  is the Lie derivative<sup>1</sup> of  $h$  along  $f$  and repeating this operator on  $L_f h(x)$  along  $g$  and  $f$ , results in  $L_g L_f h(x)$  and  $L_f^2 h(x)$ , respectively. We assume  $L_g L_f h$  is invertible. With regulation of the output to zero, the investigation of the internal stability which is performed by analyzing the internal dynamics, reduces to the zero dynamics [30]. Here, we use a  $PD$  controller ( $v$  in (3)) to obtain input-output stability. Let  $\eta := [h(q); L_f h(q)]$ ; using a diffeomorphism transform  $T$ , the normal form can be computed with new variables  $z := [\eta; \xi] = T(x)$

$$\begin{aligned} \dot{\eta} &= \begin{bmatrix} 0 & I \\ 0 & 0 \end{bmatrix} \eta + \begin{bmatrix} 0 \\ I \end{bmatrix} (L_g L_f h(x)u + L_f^2 h(x)) \\ \dot{\xi} &= f_i(\eta, \xi), \end{aligned} \quad (4)$$

in which,  $x$  will be replaced by  $T^{-1}(z)$  and  $f_i(\eta, \xi)$  describes the internal dynamics. On the zero dynamics manifold  $\mathcal{Z} := \{z | \eta = 0\}$ , the internal dynamics (the second subsystem in (4)) is simplified to the zero dynamics  $\dot{\xi} = f_0(\xi)$  where  $f_0(\xi) := f_i(0, \xi)$  (see [19] for details).

#### Definition 1: Hybrid Zero Dynamics (HZD)

Consider the hybrid model (2) and  $\dot{\xi} = f_0(\xi)$  for the zero dynamics of the swing mode, if zero dynamics manifold  $\mathcal{Z}$  is hybrid invariant; meaning

$$\Delta(\mathcal{S} \cap \mathcal{Z}) \subset \mathcal{Z} \quad (5)$$

then the hybrid zero dynamics of (2) is given by

$$\Sigma_0 := \begin{cases} \dot{\xi} = f_0(\xi), & \xi^- \notin \mathcal{S} \cap \mathcal{Z} \\ \xi^+ = \Delta(\xi^-) & \xi^- \in \mathcal{S} \cap \mathcal{Z} \end{cases} \quad (6)$$

Satisfying the hybrid invariance condition (5), the stability of the HZD as a low dimensional system (related to the degree of underactuation) results in stability of the full model [25]. Computing the normal form and evaluating it on  $\mathcal{Z}$ , results in zero dynamics equations. To analyze the stability of HZD, contact with Poincaré section which results in Poincaré map is utilized [19]. With this technique, the stability analysis is restricted to the investigation of the one dimensional discrete system, generated by the Poincaré map. For this, the states of

<sup>1</sup>See [29] for description about feedback linearization and definitions, e.g., the Lie derivative

zero dynamics can be written as  $\xi = [\xi_1, \xi_2]^T$ . Then, the zero dynamics will be give by

$$\begin{cases} \dot{\xi}_1 = \kappa_1(\xi_1)\xi_2 \\ \dot{\xi}_2 = -\kappa_2(\xi_1) \end{cases} \quad (7)$$

As suggested in [19], we define new variables  $[\zeta_1, \zeta_2] = [\xi_1, \xi_2^2/2]$  which summarizes the zero dynamics stability analysis to the stability of the discrete map  $\rho(\cdot)$  presented by

$$\rho(\zeta_2^-) = \delta_{zero}\zeta_2^- + V_{zero}(q_2^-) \quad (8)$$

This Poincaré map finds the the new variable ( $\zeta_2^-$ ) at pre-impact moment of each step, from its previous value. In this equation,  $\delta_{zero}$  is a positive value that demonstrates the impact effect for the new state variable ( $\zeta_2^- = \delta_{zero}\zeta_2^+$ ) and  $V_{zero}(q_2)$  is calculated by integrating  $\frac{d\zeta_2}{d\xi_1}$  from post impact leg angle to  $q_2$  as follows:

$$V_{zero}(q_2) = \int_{q_2^+}^{q_2} \frac{\kappa_2(q)}{\kappa_1(q)} dq \quad (9)$$

Assume  $V_{Zero}^{Max} = \max_{q_2^+ \leq q_2 \leq q_2^-} V_{zero}(q_2^-)$ ; if the following condition is satisfied,

$$C_1 \equiv \zeta_2^+ - V_{zero}^{Max} > 0, \quad (10)$$

then  $\zeta_2^-$  can be calculated by

$$\zeta_2^- = \zeta_2^+ - V_{zero}(q_2^-). \quad (11)$$

Analyzing slippage equations during the swing phase and at impact besides the above discussions summarizes the stability conditions in periodic walking with HZD controller in the next Theorem (see [19] for proofs).

*Theorem 1:* Consider the model presented by Equation (2) satisfying conditions (5) and (10), then the bipedal walker with HZD controller defined by (3) has a stable periodic motion, if and only if all the following conditions are satisfied:

$$0 < \delta_{zero} < 1 \quad (12)$$

$$C_2 \equiv \frac{\delta_{zero}}{1 - \delta_{zero}} V_{zero}(q_2^-) + V_{Zero}^{Max} < 0 \quad (13)$$

$$C_3 \equiv \delta_{zero}\zeta_2^- - V_{Zero}^{Max} > 0, \quad (14)$$

$$\frac{F^T}{F^N} > \mu_s, \quad F^N > 0 \quad (15)$$

□

In condition (15) which prevents slipping,  $\mu_s$ ,  $F^T$  and  $F^N$  are the friction coefficient, the tangential and normal forces at the foot contact with the ground, respectively. Violating Eq (14) means that the robot does not spend enough energy to finish a step successfully [19]. Our theoretical description of the proposed method (presented in the following sections) is based on this theorem.

The final step in designing the controller is determining the virtual constraints. For this, we formulate the output as the difference between the targeted variable (e.g.,  $q_1$  in Acrobot model) and the desired function ( $h_d$ ) of the guiding variable ( $q_2$  in Acrobot). Then, defining virtual constraints is restricted to the design of  $h_d(q)$ . The Bézier polynomial is commonly

used to approximate the virtual constraints [22], [25] and [31]. In Acrobot with only one actuator, the output can be defined with a holonomic constraint  $y = h(q) = q_1 - h_d(q_2)$  and the quadratic polynomial is sufficient for defining  $h_d$ . To meet the condition presented in (5), two coefficients of this polynomial are computed. From the hybrid invariance condition (5), the quadratic polynomial for virtual constraint will have the following formalism.

$$h_d(q_2) = \alpha_1 q_2^2 + 2q_2 - \alpha_1 q_2^{+2} \quad (16)$$

The remained parameter  $\alpha_1$  is used to satisfy the stability conditions in Theorem 1. As described before, after satisfying the stability conditions resulted from Poincaré map analysis, there are still parameters to be selected mostly by optimization approaches. We select the integral of the squared consumed torque  $u(t)$ , divided by the traveled distance ( $d$ ) in one step period ( $T$ ) to minimize energy consumption

$$J = \frac{1}{d} \int_{t_0}^{t_0+T} \|u(t)\|^2 dt \quad (17)$$

### III. DESIGNING A COMPLIANT HZD CONTROLLER

In this section, the design of the controller and determining the proper parallel compliance are explained as a single problem. In [19], reconfigurability of the controller is mentioned as the most significant preference of the virtual constraints rather than the physical ones. Furthermore, insertion of the compliance as a physical constraint adds many useful advantages in motion performance like increasing robustness, reducing energy consumption and fast recovery after disturbances, [32], [33], [34], [35] and [8].

We exploit the benefits of both methods by designing the controller based on virtual constraints and changing model dynamics with entering different types of compliance in the joint. In the design of our *HPC controller* (see Sec.III-D), the model without uncertainty is called *nominal model*.

#### A. Uncertainties and robustness range

In order to explain the design steps of the HPC controller, we introduce *uncertainty* and *robustness range*.

**Definition 2:** *Uncertainty range*  $\mathcal{P}$  is defined as the range for the uncertain parameter values  $p$  to cope with (e.g., downhill ground slope upto  $10^\circ$  gives  $\mathcal{P} = [0 \ 10]$ ). This range is defined such that for every parameter set  $p \in \mathcal{P}$ , there exists at least one HZD controller that results in stable walking. All controllers must have the same virtual constraints (the function of  $h(q)$ ). For a parameter set  $p \in \mathcal{P}$ , subindex  $p$  is utilized to show the related functions, matrices and vectors (e.g.,  $D_p$  for inertia matrix using parameter set  $p$ ).

**Definition 3:** *Norm, distance and neighborhood*  
The norm used in this paper is “2-norm”. The distance of two vectors  $v_1$  and  $v_2$  is defined by  $\|v_1 - v_2\|$ . Distance to a manifold for a point  $p \in \mathbb{R}^n$  to a manifold  $\mathcal{M} \in \mathbb{R}^n$  is  $|p|_{\mathcal{M}} = \inf_{m \in \mathcal{M}} \{\|m - p\|\}$ . For a manifold  $\mathcal{M} \in \mathbb{R}^n$  and positive constant  $\epsilon$ , subset  $\mathcal{N}(\mathcal{M}, \epsilon) = \{p \in \mathbb{R}^n \mid |p|_{\mathcal{M}} \leq \epsilon\}$  is called the  $\epsilon$ -neighborhood of manifold  $\mathcal{M}$ .

Consider the normal form (4) with addition of model uncertainty in which the real model is different from the

nominal model. It is shown that after feedback linearization with controller (3), the system will have *matched uncertainty*<sup>2</sup> [30], [29];  $\delta(z)$ , as follows

$$\begin{aligned} \dot{\eta} &= \underbrace{\begin{bmatrix} 0 & I \\ -K_P & -K_D \end{bmatrix}}_{A_c} \eta + \underbrace{\begin{bmatrix} 0 \\ I \end{bmatrix}}_b \delta(z) \\ \dot{\xi} &= f_i(\eta, \xi) \end{aligned} \quad (18)$$

**Lemma 1:** Consider system (18), where  $A_c$  is Hurwitz and  $\xi^*$  is the zero-invariant set<sup>3</sup> of the internal dynamics  $\dot{\xi} = f_i(\eta, \xi)$ . Suppose that  $\xi^*$  is the asymptotically stable manifold of the zero dynamics and the uncertainty  $\delta(z)$  satisfies

$$\|\delta(z)\| \leq \gamma \|\eta\| + \epsilon \quad (19)$$

for non-negative constants  $\gamma$  and  $\epsilon$ . For every  $\epsilon_M > 0$ , a neighborhood  $\mathcal{D}$  around  $z^* = [0; \xi^*]$ , matrices  $K_P$  and  $K_D$  and time  $t_0$  can be found such that,

$$\|z(t)|_{z^*} \leq \epsilon_M, \forall t \geq t_0, \forall z(0) \in \mathcal{D}. \quad (20)$$

□

The derivation of (18) and the proof of lemma 1 are described in [23]. This Lemma is presented for the continuous system (18) and we extend it to hybrid systems in the following section. We assume that the uncertainty  $\delta$  is bounded which is a reasonable requirement that follows from continuous differentiability of the nonlinear functions [29]. This upperbound does not have a direct relation to  $\xi$ . This means that the influence of  $\xi$  (and higher orders of  $\eta$ ) on the uncertainty are considered in  $\epsilon$ .

**Definition 4:** In a bipedal walking model stabilized by HZD controller (3), the *robustness range* is defined by  $(\epsilon^*, \gamma^*)$  for which the matched uncertainties  $\|\delta\| \leq \gamma^* \|\eta\| + \epsilon^*$  cannot destabilize the controlled system.

**Definition 5:** Maximum impact of uncertainty on HZD is defined by the infinite norm of the decoupling matrix for the uncertain system on the zero dynamics manifold as follows

$$U_p = \sup_q \left\| \frac{\partial h}{\partial q} D_p^{-1} B|_z \right\|. \quad (21)$$

In addition, we find 'the uncertainty bias upper limit' by the following equation

$$U_m = \sup_{p \in \mathcal{P}} U_p, \quad (22)$$

This relation means that the bias term of uncertainty ( $\epsilon$  in (19)) has an upper limit. In other words, the growth of the matched uncertainty is not faster than a linear function of  $\eta$ .

### B. Increasing robustness with parallel compliance

In this section, it is shown that addition of appropriate compliance parallel to the actuators could preserve stability in a wide range of parameters variations. Accordingly, a design methodology will be presented in the next section.

<sup>2</sup>The uncertain terms enter the state equation at the same point as the control input.

<sup>3</sup>A zero-invariant set  $\mathcal{A}$  for a system  $\dot{x} = f(x, u)$  is an invariant set of the unforced system  $\dot{x} = f(x, 0)$ , meaning  $x_0 \in \mathcal{A} \Rightarrow x(t, x_0, 0) \in \mathcal{A}, \forall t > 0$ .

For modelling an additional torque vector ( $\tau_c(q, \dot{q})$ ) that is produced by the joint compliance (parallel to the actuators),  $u$  in (1) should be replaced by  $u + \tau_c$ .

**Definition 6:** For the two matrices  $K_P$  and  $K_D$  with largest singular values  $\bar{K}_P$  and  $\bar{K}_D$ , respectively, we define the control gain  $K_{PD}$  as follows

$$K_{PD} := \frac{\bar{K}_P \bar{K}_D}{\bar{K}_P + \bar{K}_D} \quad (23)$$

**Theorem 2:** Consider the bipedal walker dynamic model (2) with the nominal parameter set  $n \in \mathcal{P}$  (called  $\Sigma_n$ ) and HZD controller  $K_n$  (producing control torque  $u_n$ ). Suppose that for a parameter set  $p \in \mathcal{P}$  different from  $n$ , a controller ( $K_p$  with control torque  $u_p$ ) using virtual constraints ( $h(x)$ ) and PD coefficients ( $K_P$  and  $K_D$ ) equal to those of the nominal model, generates stable walking for the uncertain system  $\Sigma_p$ . If there exists positive  $\epsilon^*$  s.t.

$$\|u_n - u_p\| \leq \frac{\epsilon^*}{\|U_p\|} \quad (24)$$

and

$$K_{PD} \geq 2\Pi_m(q) \|u_n - u_p\| \quad (25)$$

in which  $K_{PD}$  is given by (23) and  $\Pi_m(q)$  is the supremum of the distance between  $L_g L_f h(q)_p$  and its projection on the zero dynamics manifold  $\mathcal{Z}$ , divided by the output  $h(q)$ . Then, the HZD controller  $K_n$  stabilizes  $\Sigma_p$ . □

**Theorem 3:** Consider the two systems ( $\Sigma_n$  and  $\Sigma_p$ ) with parameter sets  $n$  and  $p$ , satisfying conditions of *Theorem 2*, except (24). Suppose that a set of compliant elements produces the additive torque vector  $\tau_c$  parallel to the actuator torque vector ( $u$ ). If

$$\begin{cases} \|\tau_c\| \leq \min(\frac{K_{PD}}{2\Pi_n}, \frac{\epsilon^*}{U_n}) \\ \|u_n + \tau_c - u_p\| \leq \min(\frac{K_{PD}}{2\Pi_p}, \frac{\epsilon^*}{U_p}) \end{cases} \quad (26)$$

then, the HPC controller  $K_c$  –comprised of  $K_n$  and compliance  $\tau_c$ – stabilizes both systems  $\Sigma_n$  and  $\Sigma_p$ . □

The proofs of the theorems are presented in the complementary paper [23]. The importance of theorem 3 is in presenting a new controller which can stabilize both systems  $\Sigma_n$  and  $\Sigma_p$  without knowing the correct parameters. When condition (24) is not satisfied, the nominal controller  $K_n$  cannot stabilize the system with uncertain parameter  $p$ , meaning that this controlled system is not robust against such an uncertainty. By adding the parallel compliance  $\tau_c$  to the actuator, deviation from nominal controller is accepted in order to increase robustness. Therefore, the HPC controller will have lower performance in the nominal case and higher robustness against uncertainties. As a result, parallel compliance can increase the robustness range upto it double size (proved in Sec. III-C).

### C. Robust HZD-based controller design

In this section, we present a method to design an HZD-based controller and in the next section we explain how to insert parallel compliance to increase robustness passively. Instead of an attractive manifold, we introduce an attractive region for satisfying boundedness in a range of parameters. Here, first we design a nominal controller  $K_n$  for all  $N - 1$  active joints

using virtual constraints that work for any  $p \in \mathcal{P}$ . Then, for each joint we modify the controller to increase the robustness as follows:

- i) Find extremes of actuation with respect to parameter  $p$   $u_{min}(q, \dot{q}) = \inf_p u_p(q, \dot{q})$ , and  $u_{max}(q, \dot{q}) = \sup_p u_p(q, \dot{q})$ .
- ii) Define the robust HZD-based controller  $K_r$  with the following control effort

$$u_r(q, \dot{q}) = \frac{u_{max}(q, \dot{q}) + u_{min}(q, \dot{q})}{2}. \quad (27)$$

Suppose that a controller  $K_c$  generates actuation  $u_c(q, \dot{q})$ . For a specific set of parameters  $p$ , let's define the maximum difference between the desired HZD controller  $u_p$  and  $u_c$  by  $\delta u_c^p = \sup_{q, \dot{q}} \|u_c - u_p\|$ . This difference shows the maximum torque to be added to controller  $u_c$  that gives the required torque  $u_p$ . The lower this difference, the less required additional torque which means that controller  $u_c$  is less different than the desired one and is more robust against uncertainties. Among the whole parameter range, The largest difference between the controller  $u_c$  and the desired HZD controllers in full information case ( $u_p$ ) can be found as  $\overline{\delta u_c} = \sup_p (\delta u_c^p)$ . Let's define,

$$du(q, \dot{q}) = \frac{u_{max}(q, \dot{q}) - u_{min}(q, \dot{q})}{2} \quad (28)$$

From definition of our robust HZD controller  $K_r$  in step (ii), we have

$$\overline{\delta u_r} = \sup_p (\delta u_r^p) = \sup_{q, \dot{q}} du(q, \dot{q}). \quad (29)$$

Therefore, the robustness range of a nominal controller  $u_n$  can be increased up to double size:

$$\overline{\delta u_r} \leq \overline{\delta u_n} \leq 2\overline{\delta u_r} \quad (30)$$

This equation shows that compared to a nominal model  $u_n$ , the norm of the difference between the produced torque and desired torque  $\overline{\delta u_n}$  is larger than that of the robust controller  $\overline{\delta u_r}$ . The ratio between these two numbers could increase up to 2 meaning that the controller  $u_r$  could be two times more robust than  $u_n$  against parameter uncertainties.

**Theorem 4:** Assume there is no nominal controller  $K_n$  satisfying condition (24) for all uncertain parameter  $p \in \mathcal{P}$ . The controller  $K_r$  given by (27) is robust against uncertainty  $p$ , if the following condition is held.

$$\|u_{max} - u_{min}\| \leq \min\left(\frac{K_{PD}}{\Pi_m}, \frac{2\epsilon^*}{U_m}\right) \quad (31)$$

□

The proof is presented in [23]. Condition (31) satisfies (24) for any uncertain parameter  $p \in \mathcal{P}$  if and only if the controller is the robust HZD controller  $K_r$ . For example, if the “ $\leq$ ” turns to “ $=$ ”, the controlled system for any HZD controller except  $K_r$  is not robust against uncertainties in the whole region. It is noticeable that the proposed robust controller  $K_r$  is not a standard HZD controller and then there is no closed form control formulation for  $u_r$ . In addition, this controller needs to compute the required torque for the uncertain parameter changing in the whole uncertain region at each instants of time which is computationally expensive. To resolve these issues, we propose a method to design a hybrid compliant controller

to benefit from advantages of producing part of the control effort by parallel passive elements.

#### D. Robust HPC controller design

In this framework the parallel compliance (PC) and the controller (HZD) are simultaneously designed resulting in a hybrid controller with mixture of virtual and physical constraints. The compliant elements are considered in the  $N - 1$  active joints. We consider a (nonlinear) function ( $\tau_c(q, \dot{q})$ ; e.g., a polynomial) of the joint angle ( $q$ ) and angular velocity ( $\dot{q}$ ). No constraint in defining compliance function  $\tau_c(q, \dot{q})$  is enforced by the HPC control design method. Therefore, any implementable impedance function can be used for  $\tau_c(q, \dot{q})$ . One step further is to design new functions which can increase robustness and then to find methods for the physical implementation. Later, we introduce one solution which is employing the pneumatic artificial muscle (PAM) as an adjustable parallel compliance. We have identified the dynamic model of PAMs [36] which can be used as nonlinear function  $\tau_c$  (tunable by the injected amount of air) to design the hybrid controller.

**Definition 7:** We assume that the walking model is controllable with a parameter dependent HZD controller  $K_p$ , if the uncertain parameter  $p \in \mathcal{P}$  is known. In such a condition, a fixed virtual constraint which is used for the controller with full information (known  $p$ ) is called ‘*stabilizing VC*’.

The goal is to design an HPC controller to work in the whole range of uncertain parameters  $p \in \mathcal{P}$ . Based on Theorem 4, there is no standard HZD controller that is robust against every  $p$  (as an uncertain parameter) in the whole region  $\mathcal{P}$ . The here presented algorithm that gives the desired compliance for each joint, includes two main parts:

*part 1: defining the nominal model*

- 1) Consider a set of parameters as the nominal model  $\Sigma_n$
- 2) Design an HZD based controller  $K_n$  for the nominal model  $\Sigma_n$  with equation (3) using the *stabilizing VC* (working for any  $p \in \mathcal{P}$ ).
- 3) Find  $u_{min}(q, \dot{q}) = \inf_p u_p(q, \dot{q})$  and  $du_p = u_p(q, \dot{q}) - u_{min}(q, \dot{q})$ .
- 4) Find  $n_{min} = \operatorname{argmin}_p \{\sup_{q, \dot{q}} du_p(q, \dot{q})\}$
- 5) If  $\Sigma_n = \Sigma_{n_{min}}$  continue, otherwise set  $\Sigma_n = \Sigma_{n_{min}}$  and jump to step 2.
- 6) Define  $u_{min}$ ,  $u_{max}$  and the robust HZD controller  $K_r$  (Eq. (27)), from steps (i) and (ii) in Sec. III-C.

Here,  $u_{min}$  and  $u_{max}$  define the variation range of the control inputs in this region of parameter changes. As aforementioned, there is no HZD controller that stabilizes the system for every uncertain parameter set  $p \in \mathcal{P}$  while parameter  $p$  is not known<sup>4</sup>. In this method, searching in the uncertain range to find extreme values are applied off-line and the computational cost is not important. Based on these two parts, finally, we introduce one HZD controller that is given with an analytical formulation plus parallel compliance and the computational cost of the proposed mixed controller is not higher than that of an HZD controller.

<sup>4</sup>The controller and the virtual constraints are designed such that  $K_p$  can control the system in the whole uncertain region  $\mathcal{P}$  if the parameter set  $p$  is known.

part 2: designing the compliance and control modification

- 1) Let  $\delta u(q, \dot{q}) = u_r(q, \dot{q}) - u_n(q, \dot{q})$  and find the parameters of the compliant structure  $\tau_c(q, \dot{q})$  to minimize  $\delta\tau := \sup_{q, \dot{q}} \|\delta u - \tau_c\|$ .
- 2) Using  $\overline{\delta u_r}$  from (29), let  $R := \overline{\delta u_r} + \delta\tau$  and  $K_{PD}$  from Definition 6; if  $K_{PD} < 2\Pi_m R$ , multiply PD gains by  $\frac{2\Pi_m R}{K_{PD}}$  and go to Step 2 of part 1
- 3) For the nominal model, find the upper bound  $\epsilon^*$  of the robustness range, based on Definition 4.
- 4) Compute  $\epsilon = RU_m$ ; if  $\epsilon > \epsilon^*$  change the compliance structure and go to Step 1.
- 5) The HPC controller  $K_c$  is defined by the controller  $K_n$  plus the compliance  $\tau_c$ .

**Theorem 5:** The HPC controller produces a stable closed-loop system for the whole uncertain region  $\mathcal{P}$ .

The proof of this theorem which is based on Theorems 2-4, is presented in [23]. The proposed algorithm provides an instruction to design a robust controller comprised of an HZD controller and a parallel compliance (PC) which is called HPC controller. In the following we describe how to use this method in two different case studies.

E. Case study 1: Acrobot model

The first case is developing a robust controller for walking with the Acrobot model on an unknown slope (uncertain parameter  $p$ ). In this model, there is one place to add parallel compliance to the actuator at hip joint and the extremes ( $u_{max}$  and  $u_{min}$ ) can be analytically computed as a function of the ground slope. Here, we describe the details of designing the HPC controller for the Acrobot model which is divided into two parts. First, the method of selecting the most robust HZD controller (without compliance) that can be obtained by changing the free parameter of the quadratic polynomial is described. Then, the effect of inserting compliant elements with different structures is explained. The superiority of nonlinear structure for increasing the robustness, which was introduced before in [37] and [38], is approved in Sec. IV. In control of the Acrobot model, the ground slope in the nominal model is set to zero (flat terrain) and different values for the slope is considered as the uncertainty to evaluate the robustness. The equations of motion are implemented within Matlab/Simulink applying the ode45 solver. The mechanical properties of the Acrobot are taken from [39].

1) *Designing a robust controller for the flat surface:* Analyzing the stability and robustness in this section is founded on Theorem 1, in which conditions (5), (10) and (12-15) should be satisfied for stable walking. As stated before, in HZD controller with quadratic polynomial, if the virtual constraint has the form presented by (16), the first condition (5) is fulfilled. The upper and lower limits of  $\alpha_1$  are determined using the other stability conditions. Assume  $q_2^+ = -13^\circ$ , the variations of the necessary conditions with respect to  $\alpha_1$  are shown in Fig. 2. On the top figure,  $V_{Zero}$  and  $\zeta_2$  are positive and  $\delta_{zero}$  is less than one for  $-23.5 < \alpha_1 < -7.5$  which are necessary conditions for stability. Additional conditions for stability are satisfied if the blue (solid) and red (dashed) curves have positive, but the black (dotted) curve negative values in

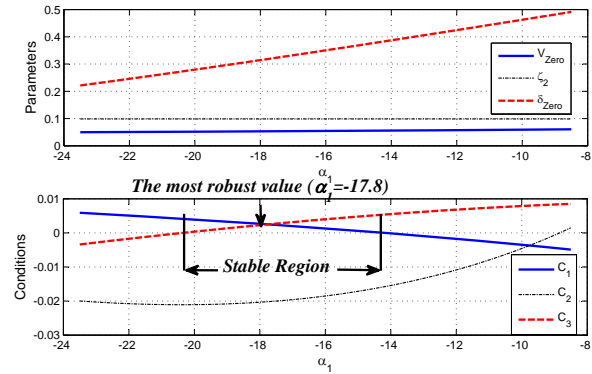


Fig. 2: The Controlled system specifications according to coefficient variation: (Top) The parameters which are needed to show the stability (Bottom) The conditions which should be checked

the bottom figure. Fig. 2 shows that only between -14.3 and -20.3 all the conditions are satisfied. This figure also depicts that the largest stability margin (the largest distance to zero) is achieved by  $\alpha_1 = -17.8$ .

2) *Compliance insertion:* Different structures for compliance are investigated to find the most effective one for walking on the widest range of slopes. The compliant element is defined as  $\tau_c = \tau_D + \tau_S$  including nonlinear (deadzone) characteristics for both spring ( $\tau_S$ ) and damper ( $\tau_D$ ) effects:

$$\tau_D = \begin{cases} 0 & \text{if } \dot{q}_1 \leq d \\ B_d \dot{q}_1 & \text{Otherwise} \end{cases} \quad (32)$$

$$\tau_S = \begin{cases} 0 & \text{if } q_1 \leq s \\ K_s q_1 & \text{Otherwise} \end{cases} \quad (33)$$

in which,  $B_d$ ,  $K_s$ ,  $d$  and  $s$  are non-negative constants and the spring rest angle is set to zero. Physical implementation of such mechanisms are possible, e.g. the seat belt is a sample of such a nonlinear damper. There is no restriction to define the nonlinear function except manufacturing feasibility.

F. Case study 2: 5-link model

In the 5-link model, the upper body is represented by a rigid trunk and each leg has two segments for thigh and shank, as shown in Fig. 1b. According to the angles demonstrated in this figure, the angle vector is defined by  $q := [q_1 \dots q_5]^T$ . The leg angle  $\varphi := \frac{3\pi}{2} - q_1 + \frac{q_3}{2} - q_5$  (shown in Fig.1b), monotonically increasing during each step, can parameterize the virtual constraints. From results of human walking pattern in [40], it is observed that the joint angles can be characterized as functions of the leg angle. In that respect, we define the outputs as follows:

$$y_i = q_i - h_d^i(\varphi), \quad i = 1..4 \quad (34)$$

in which  $h_d^i(\cdot)$ s are polynomials of degrees smaller than 4. After satisfying the stability conditions, the polynomial coefficients are set to generate trajectories similar to the joint angles in human gaits [40]. By adopting the model parameters from

human segment data [41] and with the HZD controller using virtual constraints (34), stable walking at different speeds (from  $0.5 \frac{m}{s}$  to  $2.6 \frac{m}{s}$ ) can be achieved [42]. Here we consider  $1.25 \frac{m}{s}$  as moderate walking speed.

The model uncertainty is defined by considering  $\pm 10\%$  deviation in the segments' lengths ( $L = [L_T, L_{th}, L_{sh}]$ , shown in Fig. 1b). This type of uncertainty affects on inertia matrix  $D$ , Coriolis matrix  $C$  and gravity vector  $G$ . There is no HZD controller that can stabilize the motion with this uncertainty range and the mentioned virtual constraints. To solve this problem, an HPC controller is developed in which the compliance structure is constructed by rotational springs with linear force-angle relations.

### G. BioBiped experimental setup

The BioBiped robot series is inspired by the muscular architecture of human leg (see <http://www.biobiped.de/index/> and [4]). In this robot series, human muscles are modeled by passive springs or SEAs (series elastic actuators). As shown in Fig. 5a, we replaced the spring of the SEA for the vastus muscle by a PAM (pneumatic artificial muscle), and to investigate the effects of a parallel compliance, we added a parallel PAM (PPAM) to the combination of EM and serial PAM (SPAM); see Fig. 5a. This configuration is called EPA (electric-pneumatic actuator) [36]. In Sec. IV-C, we present the experimental results of controlling the knee joint in quiet standing condition and we show how adjustment of PPAM compliance (through tuning air pressure) can be used for efficient motion control.

In this experiment, we fix the robot trunk orientation by a rigid frame (see [43] for details about this arrangement) while the controlled leg is moving freely (similar to swing leg motion in walking). We also employ the knee actuator to generate a periodic movement at different frequencies. The desired joint position is given by a sinusoidal signal, in which the frequency is increasing linearly from  $0.5Hz$  to  $2Hz$  in 5 minutes. For 3 different pressure values of SPAM we investigate the effect of the parallel compliance on energy consumption by comparing no PPAM with PAM pressure of  $145kPa$  and  $170kPa$ . The integrated square of electric current  $I$  in the period of the sinusoidal signal  $T$  was used as a measure of energy consumption while the movement patterns are kept similar.

$$E = \int_T I^2 dt \quad (35)$$

As the voltage is similar for all cases, the current can be used to define a measure ( $E$ ) for energy consumption. It is shown that using an appropriate compliant element can result in reducing energy consumption for doing a specific periodic movement. Such an adjustable compliant element can be used in our proposed HPC controller to increase both robustness and efficiency.

## IV. RESULTS

### A. Simulations: Acrobot model

As described in Sec. III-E, the nominal model is walking on flat surface. Then, the maximum slope that a fixed HZD

controller can stabilize the walker on (without knowing the slope) is  $5^\circ$ . Here, we present robustness improvement with increasing compliance structure complexity.

1) *Linear Damper*: When linear spring does not improve the motion regarding our target, the first choice is a linear damper. The highest slope that is stabilizable with addition of a linear damper is  $7^\circ$  when ( $B_d = 0.2$ ). Compared with the rigid robot, it is qualified to make a periodic walking which satisfies the stability conditions on slightly steeper terrains. Larger coefficients disturb the motion on the flat surface and result in insufficient energy to finish steps successfully.

2) *Linear Damper and Linear Spring*: When the spring is added to the robot, the allowable range for damper coefficient raises. With  $K_s = 13$  and  $B_d = 1$ , the robot can move stably on slopes between  $0^\circ$  and  $10^\circ$ . Insertion of linear damper and spring does not perturb the limit cycles and the smoothness is preserved. In addition, stable walking with higher speeds is attainable with more energy consumption.

3) *Nonlinear Damper*: A considerable robustness improvement is gained using a nonlinear damper. One of the most significant advantages of using the nonlinearity is preserving the quality of the motion on the flat surface as much as possible. The nonlinear damper promotes the robot walking robustness to be stable in  $17^\circ$  slope without considerable influence on walking performance on the flat surface.

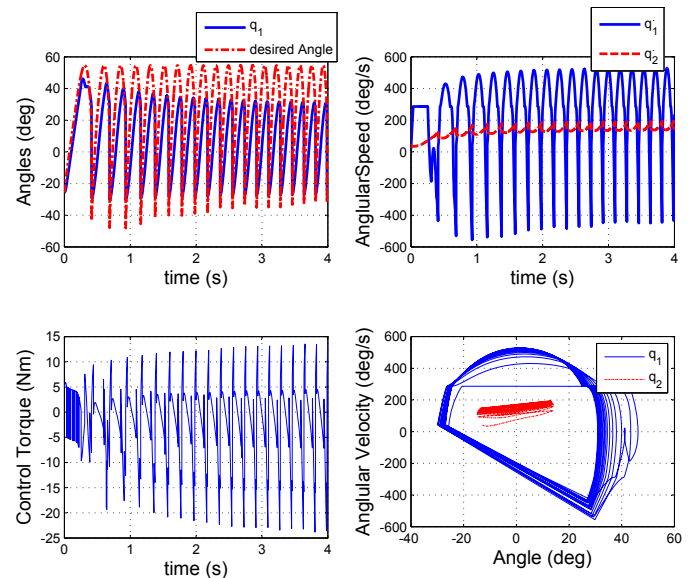


Fig. 3: The specifications of walking on slope  $20^\circ$  with the nonlinear damper  $B_d = 2$ ,  $d = 5$  and the nonlinear spring  $K_s = 13$ ,  $s = 0.75$ .

4) *Nonlinear Damper and Nonlinear Spring*: The last type of compliance is the combination of a nonlinear damper and a nonlinear spring. This is the most complex mechanism with the best performance. Utilizing this passive structure, the controller qualifies to make a stable walking on slopes up to  $20^\circ$ ; as shown in Fig. 3. In this figure, it is observed that after converging to the limit cycle, the steps will be very short and fast. Indeed, it does not yield uncontrollable angular velocities which may result in slippage or falling down. Despite existence of non-smooth trajectories in phase

TABLE I: Walking Performance using HZD controllers with different types of compliances. The traveled distance is considered for 4 seconds.

Damper ( $B_d, d$ )	Spring ( $K_s, s$ )	Energy	Speed	Distance	Slope
—	—	12.52	1.2	4.35	$5^\circ$
Lin (0.2, 0)	—	12.87	1.37	5.05	$7^\circ$
Lin (1, 0)	Lin (13, 0)	18.94	1.87	6.66	$10^\circ$
Non (2.1, 5)	—	21.33	2.15	7.76	$17^\circ$
Non (2, 5)	Non (13, 0.75)	27.78	2.46	8.73	$20^\circ$

plane at the beginning of the motion, the limit cycle is almost smooth that means less impacts and losses after convergence to the periodic solution (Fig. 3. bottom-right).

The performance of different mechanisms are compared in Table I. The consumed energy (computed by (17)) increases with respect to the slope elevation. It means that for downward slopes above  $7^\circ$ , significant increase in required energy is observed. These results are similar to the experimental findings in human locomotion [44]. At the maximum slope of  $20^\circ$ , our model predicts a walking speed of about  $2.5m/s$ .

### B. Walking robustness with 5-link model

In the simulation model of Acrobot, we considered uncertainty in the environment, modelled by unknown ground slope. Here, a second family of modelling uncertainties is addressed by error in body parameters. There is no HZD controller that can stabilize the motion with this uncertainty range. The robot may fall or slip when the controller employs uncertain parameters. To solve this problem, an HPC controller is developed in which the compliance structure is constructed by rotational springs with linear force-angle relations. We define the nominal model with the parameter set  $L_n = 0.9L$  (resulting in  $u_n = u_{min}$ ), and the worst case by  $L_w = 1.1L$  which means  $u_w = u_{max}$ . Fig. 4 shows the joint torques of the 5-link model explained in Sec. III-F. It is observed that addition of compliance compensates shortage of the control torque in the nominal controller, which is required for stabilization of the worst case model.

TABLE II: 5-link model parameters with human body characteristics [41]

Name	Parameter	value	unit
$M_T$	Torso mass	54	kg
$M_{th}$	Thigh mass	8	
$M_{sh}$	Shank mass	5	
$L_T$	Torso length	0.89	m
$L_{th}$	Thigh length	0.5	
$L_{sh}$	Shank length	0.5	
$l_T$	Hip to torso CoM distance	0.33	m
$l_{th}$	Hip to thigh CoM distance	0.21	
$l_{sh}$	Knee to shank CoM distance	0.3	
$I_T$	Torso inertia	10.6	$kgm^2$
$I_{th}$	Thigh inertia	1.8	
$I_{sh}$	Shank inertia	1	
$g$	Gravitational acceleration	9.81	$m/s^2$
$\mu$	Static friction coefficient	0.6	—

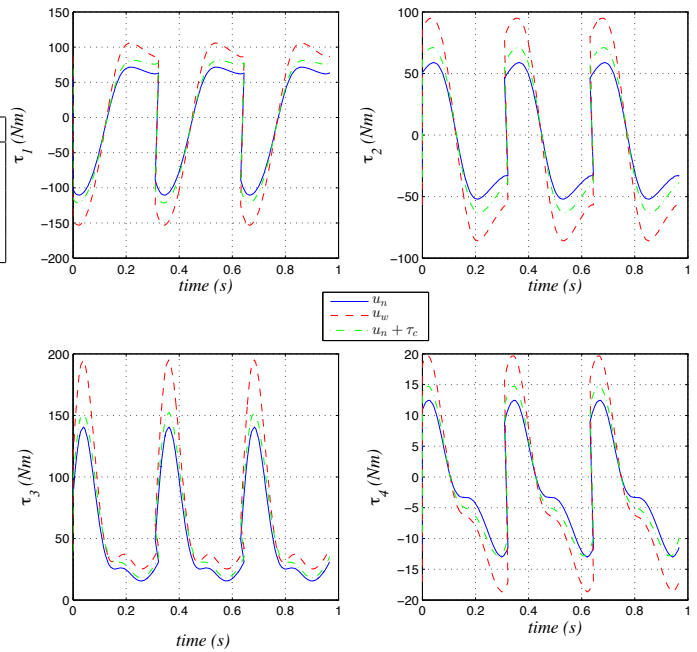


Fig. 4: Comparison between different controllers' actuations on model with 10% uncertainty in segments' lengths.  $u_n$  is nominal HZD controller ( $L_n = 0.9L$ ), and  $u_w$  is HZD control torque knowing the uncertain parameter ( $L_w = 1.1L$ ) and  $u_n + \tau_c$  is the control torque of the HPC controller.

### C. Hardware experiments

With the BioBiped3 robot (Sec. III-G), effects of parallel compliance at different frequencies are shown in Fig. 5b for 3 different pressure values of SPAMs. For each SPAM pressure value, the normalized saved energy ( $S$ ) is defined by the difference between the consumed energy (calculated by (35)) of that trial ( $E_p$ ) and the energy of the one from the same group without PPAM ( $E_0$ ) as follows.

$$S = \frac{E_p - E_0}{E_0} \quad (36)$$

Positive  $S$  values with nonzero PPAM indicate that adding parallel compliance reduces energy consumption. In addition, unlike the middle figure, in the left and right figures, the higher PPAM compliance results in a more efficient actuator. Therefore, by introducing a constant parallel compliant structure not only robustness (see Sec. IV-A and Sec. IV-B), but also energy efficiency can be improved. Therefore, with adjustable parallel compliance like the proposed EPA, both efficiency and robustness can be obtained simultaneously for a wide range of gait conditions (e.g., step frequency, speed and slope).

## V. DISCUSSION

In this paper, we studied the role of parallel compliance for improving robustness and efficiency in bipedal locomotion. We proposed a design and control approach to benefit from both virtual and physical constraints for robot walking in different walking conditions. In the literature, compliant elements are mostly used for increasing efficiency [22], [45], [46], [47]. In contrast, here we additionally focused on robustness against



uncertainties in body and environmental conditions as well. With adding parallel elastic elements, stability in larger parameter regions can be achieved without additional need for sensor-based adaptations. Adding parallel compliance not only can decrease peak torque and energy consumption [11], [12], but also can reduce the need for further sensory feedback.

One important target in design and control of legged robots is minimizing the efforts required to create walking gaits [48]. Following the mechanical design principles for passive dynamic walking (PDW) [49], bipedal gaits can emerge purely from the natural dynamics of the legs without extra torques. The resulting motions look elegant and human-like. Similarity between human walking and PDW swing leg movement suggests that humans exploit their natural dynamics with minimized amounts of energy. Although PDWs are not very stable, Collins et al. developed a bipedal robots that can walk based on this design concept [32], [50] on a flat surface. To compensate the missing robustness and versatility of PDW, optimal control methods can be utilized [51], [48]. Based on the idea of PDW, we have shown that the mechanical design (e.g. leg compliance and foot curvature) and the matching control are important at the same time for developing an energy efficient robot with human-like walking [15]. This concept of *control embodiment* [52] is based on high coupling between mechanical design and control [46]. In [15], we have implemented the HZD controller on the springy Acrobot with curved feet (SACF) model as an instance of control embodiment for bipedal walking. Indeed, the mechanical design features (springs, curved feet) and the active components (motors) were acting in series (not like here in parallel). The predicted design advantages (e.g. foot curvature) are in line with findings in human walking [53]. Instead of applying mechanical design modifications (knee and ankle, through leg spring and curved feet, respectively) and the controller (at hip joint by hip actuation) in [15] at different places, in the here presented study we implemented both mechanical and control design at the same joints. As a result, we extend the PDW concept by adding parallel compliant elements. This helped make the system dynamics robust and efficient, or more human-like. It means that by adding parallel compliance and with adjusting the system dynamics to the desired gait condition, a robust version of passive dynamic walking paradigm is provided that can be optimally controlled. The robustness is analytically guaranteed as the HZD controller and the parallel compliance are designed simultaneously.

The advantages of the parallel elasticity like reducing the required peak power and energy consumption motivates reinforcing SEAs with PEAs [54], [55], [56], [16]. This additional elements could potentially increase control complexity. To prevent more complication, we presented the HPC control method in a dynamical model with one degree of underactuation. However, this method can be applied to systems with higher degrees of underactuation (e.g. in BioBiped robot). This property is inherited from HZD controller [24], [15] because adding parallel (not serial) passive elements does not change degrees of underactuation.

By defining the function of the parallel compliant elements we shape the movement solutions by relating them to a

submanifold. An appropriate characterization of the compliant elements regarding maximizing robustness can be found using the HZD control approach. We showed that different combinations of linear and nonlinear springs and dampers can increase the robustness against ground slope while nonlinear elements are more effective. This is in line with other studies which successfully implemented nonlinear compliant elements in biped robots [57][37]. In addition, the significant role of nonlinear compliance has been illustrated in biological systems, e.g. [40] [58].

Recently, different methods were developed for constructing nonlinear compliance [11]. For example, using a specific cam pattern, nonlinear stiffness can be implemented mechanically [59]. In another study, Secer and Saranlı suggested three approaches to develop adjustable damping elements [60]. Appropriate implementation of nonlinear compliance could also result in attaining both energy consumption minimization and increasing locomotion speed [61]. Our method is not restricted by the structure of the compliant elements. Therefore, in addition to increase of robustness, reducing energy consumption and improving locomotion speed are expected.

One disadvantage of using parallel compliance might be that optimizing it for one particular task avoids achieving efficiency or effectiveness in other tasks. In the biological actuator, an adjustable parallel spring mechanism can be found by the titin filaments that can attach to actin depending the activation dynamics of the muscle (a first mathematical model was provided in [13]). Inspired by this adaptation, our suggested variable compliant elements using pneumatic actuators (described in Sec. IV-C) could help resolve the aforementioned issue. Therefore, by tuning the air pressure the optimized compliance will provide both efficiency and robustness for a range of motion conditions. Our preliminary results of implementing PAMs as parallel compliance (EPA design) on BioBiped3 robot introduces them as appropriate adjustable parallel compliance. In the future, we will apply the EPA concept on more joints of the robot for increasing robustness and efficiency in a complete gait.

#### ACKNOWLEDGMENT

This research is supported partially by the German Research Foundation (DFG) under grants No. AH307/2-1 and SE1042/29-1.

#### REFERENCES

- [1] G. A. Pratt and M. M. Williamson, "Series elastic actuators," in *Intelligent Robots and Systems '95: Human Robot Interaction and Cooperative Robots*, Proceedings. 1995 IEEE/RSJ International Conference on. IEEE, 1995, pp. 399–406.
- [2] D. W. Robinson, J. E. Pratt, D. J. Paluska, and G. A. Pratt, "Series elastic actuator development for a biomimetic walking robot," in *Advanced Intelligent Mechatronics, 1999. Proceedings. 1999 IEEE/ASME International Conference on*. IEEE, 1999, pp. 561–568.
- [3] J. Pratt and B. Krupp, "Design of a bipedal walking robot," in *SPIE defense and security symposium*. International Society for Optics and Photonics, 2008, pp. 69 621F–69 621F.
- [4] K. Radkhah, C. Maufroy, M. Maus, D. Scholz, A. Seyfarth, and O. von Stryk, "Concept and design of the biobiped1 robot for human-like walking and running," *International Journal of Humanoid Robotics*, vol. 8, no. 03, pp. 439–458, 2011.

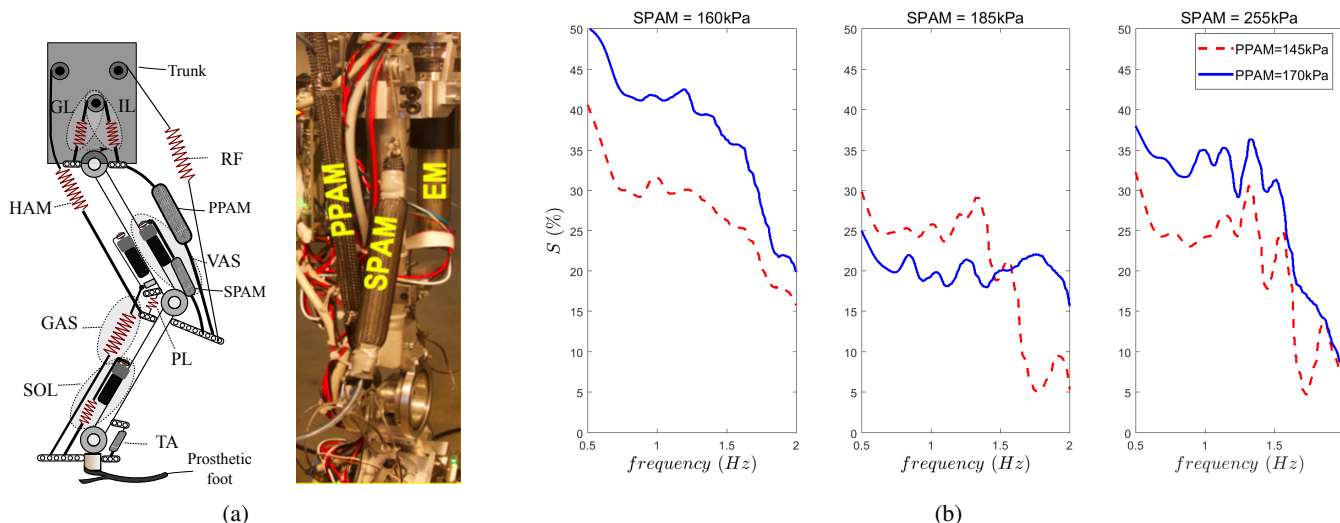


FIG. 5: (a) Implementation of parallel compliance using PAM in BioBiped3 representing the vastus muscle, including one electric motor (EM), one serial (SPAM) and one parallel PAM (PPAM). (b) Experimental results. The desired joint position is a sinusoidal wave with frequency linearly increasing from  $0.5\text{Hz}$  to  $2\text{Hz}$ , over a period of 5 minutes. The approximation of saved energy ( $S$ ) compared to no PPAM case is shown for different PAM pressures and oscillations frequencies.

[5] J. E. Pratt and B. T. Krupp, "Series elastic actuators for legged robots," in *Defense and Security*. International Society for Optics and Photonics, 2004, pp. 135–144.

[6] M. Grimmer, M. Eslamy, and A. Seyfarth, "Energetic and Peak Power Advantages of Series Elastic Actuators in an Actuated Prosthetic Leg for Walking and Running," *Actuators*, vol. 3, no. 1, pp. 1–19, Mar. 2014.

[7] P. V. Komi, "Stretch-shortening cycle," *Strength and power in sport*, vol. 3, pp. 184–202, 2008.

[8] J. W. Hurst, "The role and implementation of compliance in legged locomotion," Ph.D. dissertation, Robotics Institute, Carnegie Mellon University, 2008.

[9] B. Vanderborght, A. Albu-Schäffer, A. Bicchi, E. Burdet, D. G. Caldwell, R. Carloni, M. Catalano, O. Eiberger, W. Friedl, G. Ganesh, and others, "Variable impedance actuators: A review," *Robotics and Autonomous Systems*, vol. 61, no. 12, pp. 1601–1614, 2013.

[10] R. Van Ham, B. Vanderborght, M. Van Damme, B. Verrelst, and D. Lefeber, "MACCEPA, the mechanically adjustable compliance and controllable equilibrium position actuator: Design and implementation in a biped robot," *Robotics and Autonomous Systems*, vol. 55, no. 10, pp. 761–768, 2007.

[11] G. Mathijssen, D. Lefeber, and B. Vanderborght, "Variable recruitment of parallel elastic elements: Series-parallel elastic actuators (SPEA) with dephased mutilated gears," *IEEE/ASME Transactions on Mechatronics*, vol. 20, no. 2, pp. 594–602, 2015.

[12] U. Mettin, P. X. La Hera, L. B. Freidovich, and A. S. Shiriaev, "Parallel elastic actuators as a control tool for preplanned trajectories of underactuated mechanical systems," *The international journal of robotics research*, vol. 29, no. 9, pp. 1186–1198, 2010.

[13] C. Rode, T. Siebert, and R. Blickhan, "Titin-induced force enhancement and force depression: a sticky-spring mechanism in muscle contractions?" *Journal of theoretical biology*, vol. 259, no. 2, pp. 350–360, 2009.

[14] P. P. Purslow, "Strain-induced reorientation of an intramuscular connective tissue network: implications for passive muscle elasticity," *Journal of biomechanics*, vol. 22, no. 1, pp. 21–31, 1989.

[15] S. Yazdi-Mirmokhalesouni, M. Sharbafi, M. Yazdanpanah, and M. Nili-Ahmadabadi, "Modeling, control and analysis of a curved feet compliant biped with hzd approach," *Nonlinear Dynamics*, vol. 91, no. 1, pp. 459–473, 2018.

[16] A. S. M. Grimmer and M. Eslamy, "A comparison of parallel and series elastic elements in an actuator for mimicking human ankle joint in walking and running," in *IEEE International Conference on Robotics and Automation (ICRA)*, 2012.

[17] F. Iida and R. Tedrake, "Minimalistic control of a compass gait robot in rough terrain," in *of the 2009 IEEE International Conference on Robotics and Automation (ICRA 2009)*, 2009, pp. 1985–1990.

[18] F. Iida, Y. Minekawa, J. Rummel, and A. Seyfarth, "Toward a human-like biped robot with compliant legs," *Robotics and Autonomous Systems*, vol. 57, no. 2, pp. 137–144, 2009.

[19] E. R. Westervelt, J. W. Grizzle, C. Chevallereau, J. H. Choi, and B. Morris, *Feedback Control of Dynamic Bipedal Robot Locomotion*. Taylor & Francis, CRC Press, 2007.

[20] I. Poulakakis, "Stabilizing monopedal robot running: Reduction-by-feedback and compliant hybrid zero dynamics," Ph.D. dissertation, University of Michigan, 2009.

[21] B. Morris and J. W. Grizzle, "Hybrid invariant manifolds in systems with impulse effects with application to periodic locomotion in bipedal robots," *IEEE Transaction on Automatic Control*, vol. 54, no. 8, pp. 1751–1764, 2009.

[22] K. Sreenath, H.-W. Park, I. Poulakakis, and J. W. Grizzle, "A compliant hybrid zero dynamics controller for stable, efficient and fast bipedal walking on mabel," *The International Journal of Robotics Research*, vol. 30, no. 9, pp. 1170–1193, 2011.

[23] M. A. Sharbafi, M. J. Yazdanpanah, M. N. Ahmadabadi, and A. Seyfarth, "Parallel compliance design for increasing robustness and efficiency in legged locomotion – theoretical background," *IEEE Transaction on Mechatronics*, under review.

[24] K. A. Hamed and J. W. Grizzle, "Iterative robust stabilization algorithm for periodic orbits of hybrid dynamical systems: Application to bipedal running," *IFAC-PapersOnLine*, vol. 48, no. 27, pp. 161–168, 2015.

[25] E. R. Westervelt, J. Grizzle, and D. E. Koditschek, "Hybrid zero dynamics of planar biped walkers," *IEEE Transactions on Automatic Control*, vol. 48, pp. 42–56, 2003.

[26] J. Grizzle, G. Abba, and F. Plestan, "Asymptotically stable walking for biped robots: Analysis via systems with impulse effects," *IEEE Transactions on Automatic Control*, vol. 46, pp. 51–64, 2001.

[27] C. Shih, J. W. Grizzle, and C. Chevallereau, "Asymptotically stable walking of a simple underactuated 3d bipedal robot," in *In Reprint 33rd Annual Conference of IEEE Industrial Electronics (IECON 2007)*, 2007, pp. 1404–1409.

[28] J. W. Grizzle, C. Chevallereau, and C. long Shih, "Hzd-based control of a five-link underactuated 3d bipedal robot," in *In Proc. of 47th IEEE Conference on Decision*, 2008.

[29] H. Khalil, *Nonlinear Systems*. Prentice Hall, 2002.

[30] A. Isidori, *Nonlinear Control Systems*, 3rd ed. Berlin: Springer-Verlag, 1995.

[31] J. Choi and J. W. Grizzle, "Feedback control of an underactuated planar bipedal robot with impulsive foot action," *Robotica*, vol. 23, no. 5, 2005.

[32] S. Collins, A. Ruina, R. Tedrake, and M. Wisse, "Efficient bipedal robots based on passive-dynamic walkers," *Science*, vol. 307, no. 5712, pp. 1082–1085, 2005.

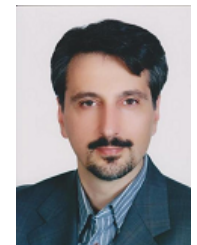
- [33] I. Thorson, M. Svinin, S. Hosoe, F. Asano, and K. Taji, "Design considerations for a variable stiffness actuator in a robot that walks and runs," in *In Proc. of the Robotics and Mechatronics Conference (RoboMec)*, 2007.
- [34] D. Owaki, M. Koyama, S. Yamaguchi, S. Kubo, and A. Ishiguro, "A 2-d passive-dynamic-running biped with elastic elements," *IEEE Transactions on Robotics*, vol. 27, no. 1, pp. 156–162, 2011.
- [35] H. Geyer, A. S. A., and R. Blickhan, "Compliant leg behaviour explains basic dynamics of walking and running," *Proceedings of the Royal Society B: Biological Sciences*, vol. 273, pp. 2861–2867, 2006.
- [36] M. Ahmad Sharbafi, H. Shin, G. Zhao, K. Hosoda, and A. Seyfarth, "Electric-pneumatic actuator: A new muscle for locomotion," vol. 6, no. 4, p. 30, 2017.
- [37] J. D. Karssen and M. Wisse, "Running with improved disturbance rejection by using non-linear leg springs," *The International Journal of Robotics Research*, vol. 30, no. 13, 2011.
- [38] M. A. Sharbafi, M. J. Yazdanpanah, and M. N. Ahmadabadi, "Compliance design in robot structure to increase the robustness," in *Dynamic Walking 2011*, 2011.
- [39] M. Garcia, "Stability, scaling, and chaos in passive-dynamic gait models," Ph.D. dissertation, Cornell University, 1999.
- [40] S. Lipfert, "Kinematic and dynamic similarities between walking and running. phd thesis," Ph.D. dissertation, University of Jena, Germany, 2010.
- [41] D. A. Winter, *BioMechanics and motor control of human movement*, 3rd ed. New Jersey, USA: John Wiley & Sons, Inc, 2005.
- [42] M. A. Sharbafi and A. Seyfarth, "Mimicking human walking with 5-link model using hzd controller," in *Robotics and Automation (ICRA), 2015 IEEE International Conference on*. IEEE, 2015, pp. 6313–6319.
- [43] M. A. Sharbafi, C. Rode, S. Kurowski, D. Scholz, R. Möckel, K. Radkhah, G. Zhao, A. M. Rashty, O. von Stryk, and A. Seyfarth, "A new biarticular actuator design facilitates control of leg function in biobiped3," *Bioinspiration & Biomimetics*, vol. 11, no. 4, p. 046003, 2016.
- [44] R. Margaria, *Sulla fisiologia e specialmente sul consumo energetico della marcia e della corsa a varie velocita ed inclinazioni del terreno*, 1938.
- [45] J. W. Hurst and A. A. Rizzi, "Series compliance for an efficient running gait," *IEEE Robotics & Automation Magazine*, vol. 15, no. 3, 2008.
- [46] P. Gregorio, M. Ahmadi, and M. Buehler, "Design, control, and energetics of an electrically actuated legged robot," *IEEE Transactions on Systems, Man, and Cybernetics, Part B (Cybernetics)*, vol. 27, no. 4, pp. 626–634, 1997.
- [47] B. Vanderborght, N. G. Tsagarakis, R. Van Ham, I. Thorson, and D. G. Caldwell, "Macepa 2.0: compliant actuator used for energy efficient hopping robot chobino1d," *Autonomous Robots*, vol. 31, no. 1, p. 55, 2011.
- [48] P. Bhounsule, "Control based on passive dynamic walking," in *Bio-inspired Legged Locomotion: Models, Concepts, Control and Applications*, M. A. Sharbafi and A. Seyfarth, Eds. Elsevier: Butterworth-Heinemann, 2017, ch. 4.6, pp. 267–291.
- [49] T. McGeer *et al.*, "Passive dynamic walking," *I. J. Robotic Res.*, vol. 9, no. 2, pp. 62–82, 1990.
- [50] S. H. Collins, M. Wisse, and A. Ruina, "A three-dimensional passive-dynamic walking robot with two legs and knees," *The International Journal of Robotics Research*, vol. 20, no. 7, pp. 607–615, 2001.
- [51] P. A. Bhounsule, J. Cortell, and A. Ruina, "Design and control of ranger: an energy-efficient, dynamic walking robot," in *Adaptive Mobile Robotics*. World Scientific, 2012, pp. 441–448.
- [52] R. Pfeifer, M. Lungarella, and F. Iida, "Self-organization, embodiment, and biologically inspired robotics," *science*, vol. 318, no. 5853, pp. 1088–1093, 2007.
- [53] P. G. Adamczyk, S. H. Collins, and A. D. Kuo, "The advantages of a rolling foot in human walking," *Journal of Experimental Biology*, vol. 209, no. 20, pp. 3953–3963, 2006.
- [54] J. Karssen, "Robotic bipedal running: Increasing disturbance rejection," Ph.D. dissertation, TU Delft, Delft University of Technology, 2013.
- [55] Y. Yesilevskiy, W. Xi, and C. D. Remy, "A comparison of series and parallel elasticity in a monopod hopper," in *Robotics and Automation (ICRA), 2015 IEEE International Conference on*. IEEE, 2015, pp. 1036–1041.
- [56] M. Eslamy, M. Grimmer, and A. Seyfarth, "Effects of unidirectional parallel springs on required peak power and energy in powered prosthetic ankles: Comparison between different active actuation concepts," in *Robotics and Biomimetics (ROBIO), 2012 IEEE International Conference on*. IEEE, 2012, pp. 2406–2412.
- [57] S. Cotton, I. Olaru, M. Bellman, T. V. der Ven, J. Godowski, and J. Pratt, "Fastrunner: A fast, efficient and robust bipedal robot, concept and planar simulation," in *IEEE International Conference on Robotics and Automation (ICRA)*, 2012.
- [58] D. F. B. Haeufle, M. Guenther, R. Blickhan, and S. Schmitt, "Proof-of-concept: model based bionic muscle with hyperbolic force-velocity relation," *Applied Bionics and Biomechanics*, vol. 9, no. 3, 2012.
- [59] H. J. Bidgoly, A. Parsa, M. J. Yazdanpanah, and M. N. Ahmadabadi, "Benefiting from kinematic redundancy alongside mono-and biarticular parallel compliances for energy efficiency in cyclic tasks," *IEEE Transactions on Robotics*, 2017.
- [60] G. Secer and U. Saranlı, "Control of planar spring–mass running through virtual tuning of radial leg damping," *IEEE Transactions on Robotics*, no. 99, pp. 1–14, 2018.
- [61] M. Khoramshahi, H. J. Bidgoly, S. Shafiee, A. Asaei, A. Ijspeert, and M. Nili, "Piecewise linear spine for speedenergy efficiency trade-off in quadruped robots," *Robotics and Autonomous Systems*, vol. 61, no. 12, pp. 1350–1359, 2013.



**Maziar Ahmad sharbafi** is an assistant professor in Electrical and Computer Engineering Department of University of Tehran and a guest researcher at the Laufflabor Locomotion Laboratory, TU Darmstadt. He received the B.Sc. at Sharif University of Technology and M.Sc., and Ph.D. degrees at University of Tehran, all in control engineering. His current research interests include bio-inspired locomotion control based on conceptual and analytic approaches, postural stability, and the application of dynamical systems and nonlinear control to hybrid systems such as legged robots and exoskeletons.



**Mohammad Javad Yazdanpanah** is a professor in the School of Electrical and Computer Engineering, University of Tehran and the director of the Advanced Control Systems Laboratory. Prof Yazdanpanah received the B.Sc., M.Sc., and Ph.D. degrees from Isfahan University of Technology, Iran, in 1986, the University of Tehran, Iran, in 1988, and Concordia University, Montreal, QC, Canada, in 1997, respectively, all in electrical engineering. His research interests include analysis and design of nonlinear/optimal/adaptive control systems, robotics, control on networks, and theoretical and practical aspects of neural networks.



**Majid Nili Ahmadabadi** is a professor in the School of Electrical and Computer Engineering, University of Tehran where he is a professor and the head of Robotics and AI Laboratory. Prof. Ahmadabadi received his B.S from Sharif University of Technology of Iran in 1990 and his M.Sc. and Ph.D. in Information Sciences from the Graduate School of Information Science, Tohoku University, Japan in 1994 and 1997, respectively. In 1997, he joined the Advanced Robotics Laboratory at Tohoku University. He served as a member of the engineering board of Iranian National Science Foundation for the period 2005–2011. His main research interests are cognitive robotics and modeling cognitive systems in addition to control of legged robots.



**Andre Seyfarth** is a professor for Sports Biomechanics at the Department of Human Sciences of TU Darmstadt and head of the Laufflabor Locomotion Lab. After his studies in physics and his PhD in the field of biomechanics, he went as a DFG Emmy Noether fellow to the MIT LegLab (Prof. Herr, USA) and the ParaLab at the university hospital Balgrist in Zurich (Prof. Dietz, Switzerland). His research topics include sport science, human and animal biomechanics and legged robots. Prof. Seyfarth was the organizer of the Dynamic Walking 2011 conference (Principles and Concepts of Legged Locomotion) and the AMAM 2013 conference (Adaptive Motions in Animals and Machines).